# REPORT DOCUMENTATION PAGE

Form Approved
OMB NO. 0704-0188



| 1. AGENCY USE ONLY ( Leave Blank) | 2. REPORT DATE | 3. REPORT TYPE AND DATES COVERED |
|---|---|---|
| | March 31, 2005 | Final Report 10/01/01-12/31/04 |

4. TITLE AND SUBTITLE

Development of a Swashplateless Rotor Using Magnetic Shape Memory Alloys

5. FUNDING NUMBERS

DAAD19-01-1-0790

6. AUTHOR(S)
Ronald N. Couch
Inderjit Chopra

7. PERFORMING ORGANIZATION NAME(S) AND ADDRESS(ES)
Department of Aerospace Engineering
3181 Glenn Martin Hall
College Park, MD, 20742

8. PERFORMING ORGANIZATION REPORT NUMBER

9. SPONSORING / MONITORING AGENCY NAME(S) AND ADDRESS(ES)

U. S. Army Research Office
P.O. Box 12211
Research Triangle Park, NC 27709-2211

10. SPONSORING / MONITORING AGENCY REPORT NUMBER

42881-EG

11. SUPPLEMENTARY NOTES

The views, opinions and/or findings contained in this report are those of the author(s) and should not be construed as an official Department of the Army position, policy or decision, unless so designated by other documentation.

12 a. DISTRIBUTION / AVAILABILITY STATEMENT

Approved for public release; distribution unlimited.

12 b. DISTRIBUTION CODE

13. ABSTRACT (Maximum 200 words)

A quasi-static model for NiMnGa magnetic shape memory alloy (MSMA) is formulated in parallel to the Brinson and Tanaka thermal SMA constitutive models. Since the shape memory effect (SME) and pseudoelasticity exist in both NiTi and NiMnGa, constitutive models for SMAs can serve as a basis for MSMA behavioral modeling. The quasi-static model for NiMnGa was characterized by nine material parameters identified by conducting a series of uniaxial compression tests in a constant field environment. These model parameters include free strain, Young's modulus, fundamental critical stresses, fundamental threshold fields, and stress-influence coefficients. These test data were used to assemble a critical stress profile that is useful for determining model parameters and for understanding the dependence of critical stresses on magnetic fields. Once implemented, the analytical model shows good correlation with test data for all modes of NiMnGa quasi-static behavior, capturing both the magnetic shape memory effect and pseudoelasticity. Furthermore, the model is also capable of predicting partial pseudoelasticity, minor hysteretic loops and stress-strain behaviors. To correct for the effects of magnetic saturation, a series of stress influence functions were developed from the critical stress profile. Although requiring further refinement, the model's results are encouraging, indicating that the model is a useful analytical tool for predicting NiMnGa actuator behavior.

14. SUBJECT TERMS
Magnetic shape memory, NiMnGa, martensite, quasi-static modeling, critical stress, pseudoelasticity

15. NUMBER OF PAGES
17

16. PRICE CODE

| 17. SECURITY CLASSIFICATION OR REPORT | 18. SECURITY CLASSIFICATION ON THIS PAGE | 19. SECURITY CLASSIFICATION OF ABSTRACT | 20. LIMITATION OF ABSTRACT |
|---|---|---|---|
| UNCLASSIFIED | UNCLASSIFIED | UNCLASSIFIED | UL |

**To:** Gary L. Anderson, Army Research Office
**From:** Ron Couch, Graduate Student, Aerospace Engineering, University of Maryland, College Park
**Subject:** Final Report on Magnetic Shape Memory Alloy Research
**Date:** March 31, 2005

## Introduction

This is the final progress report related to the magnetic shape memory alloy (MSM) research currently being conducted at the University of Maryland. The characterization and modeling of the quasi-static and dynamic behavior NiMnGa MSM alloy is the current focus of research. Our goal is to determine the response of NiMnGa to a wide range of magnetic and mechanical loading conditions. Using these data a phenomenological model that predicts the state of the MSMA for any set of quasi-static loading conditions has been developed. This model is based upon the Tanaka and Brinson models used to predict NiTi SMA behavior due to similarities that exist between both types of materials.

Magnetic fields on the order of 2 kOe applied to the FSMA actuator, can induce plastic strain recovery of up to 10%, although 6-8% strain is more typical. One of the key advantages of magnetic shape memory alloys is that its large strain recovery occurs over a wide bandwidth, reported to be well into the kHz range. In contrast, thermally driven SMAs like NiTi, have a very small bandwidth, no more than 1 Hz in ideal conditions due to the time involved with heating and cooling. Therefore, FSMAs show much more potential for applications requiring a high dynamic stroke.

Magnetically induced strains in NiMnGa alloy are the direct result of the rearrangement of the martensite twin structure of the material. At the high temperature, austenite state, NiMnGa has a cubic lattice unit cell structure. When cooled to the martensite phase, the unit cell reverts to a tetragonal configuration consisting of a long axis (a-axis) and a short axis (c-axis). Furthermore, this martensite phase is subdivided into two primary variants: a field preferred and a stress preferred state. The c-axis is aligned parallel to the axis of magnetization, also known as the 'easy' axis. Like any ferromagnetic material, the axis of magnetization will align itself with the direction of an applied external field. In magnetic shape memory alloys like NiMnGa, this process is not easily accomplished because the material exhibits a high degree of magnetocrystalline anisotropy. The effect of this anisotropy is to rigidly fix the axis of magnetization within the unit cell. Therefore, when an external field is applied to the actuator, the entire unit cell itself, tends to rotate to align the easy axis with the field direction. This process of unit cell realignment causes the material to grow field preferred twin variants at the expense of stress preferred twin

variants. When the NiMnGa specimen transitions from a stress preferred to field preferred configuration, a change in dimensions occurs. This change in actuator dimension is known as the magnetic shape memory (MSM) induced strain.

For a typical bar shaped NiMnGa actuator, an external magnetic field induces axial strain perpendicular to the direction of the applied field. The magnetic field causes twin boundary mobility resulting in an induced strain that remains when the field is removed. Induced strain may be removed by applying an axial, compressive stress to the actuator along the direction of strain. When an FSMA in the stress preferred configuration is exposed to a sufficient magnetic field at zero stress (>3.5 kOe), twin boundary motion occurs causing the actuator to become "detwinned" martensite and achieve a free strain of approximately 6%. This new configuration is the field preferred configuration. To recover the induced strain, an axial compressive load on the order of 3 to 4 MPa applied to the bar at zero applied field, reorders the twin variants and converts the actuator to its original, stress preferred configuration. This phenomenon is the magnetic shape memory effect (MSME).

Ferromagnetic shape memory alloys like NiMnGa exhibit behavior similar to conventional, thermally reactive SMAs, like NiTi. Both materials exhibit the shape memory effect and pseudoelastic behavior. The obvious difference between the two is that NiTi requires a thermal field and NiMnGa requires a magnetic field for actuation. Figure 1(a) represents an example of the MSME as observed from constant applied field experiments. NiMnGa also exhibits pseudoelastic behavior. In this case, the material, initially in the field preferred configuration, is exposed to a large magnetic field, on the order of 6 kOe. Then the specimen is subjected to increasing, axial, compressive stress large enough to change the configuration from field to stress preferred. This change in configuration induces a large plastic strain that is completely recovered in a hysteresis loop upon removal of the stress. Figure 1(b) shows an example of magnetic pseudoelasticity from experimental data.

NiMnGa also exhibits an interesting behavior at low magnetic fields. At low fields the NiMnGa can exhibit partial pseudoelastic recovery. In this case, a specimen, initially in the field preferred configuration, is subject to a small applied magnetic field of about 2 to 3 kOe. While the field remains constant, an increasing, compressive, axial stress is applied to the actuator. When the stress is removed, only a portion of the strain is recovered in the resulting hysteresis loop. Under these conditions, the

magnetic field is insufficient to induce full twin boundary mobility along the entire length of the actuator. Therefore, only a partial amount of strain is recovered. The remaining, residual strain can only be recovered by raising the level of the field to a level that activates twin boundary motion along the entire length of the actuator. In Figure 2, an experimental example of this mode of behavior occurring at a 2 kOe applied field is shown.

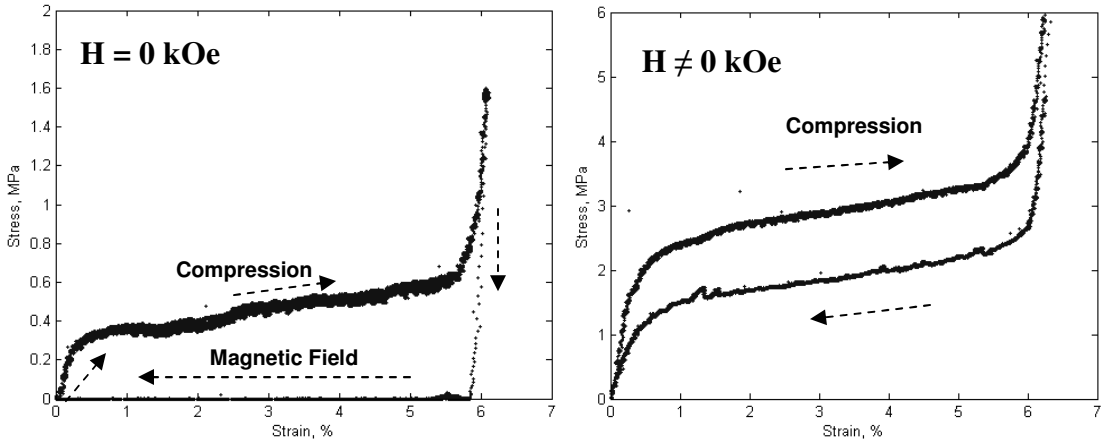


**(a) Magnetic Shape Memory Effect** **(b) Magnetic Pseudoelasticity**

**Figure 1. Primary strain recovery mechanisms in NiMnGa magnetic shape memory alloy.**

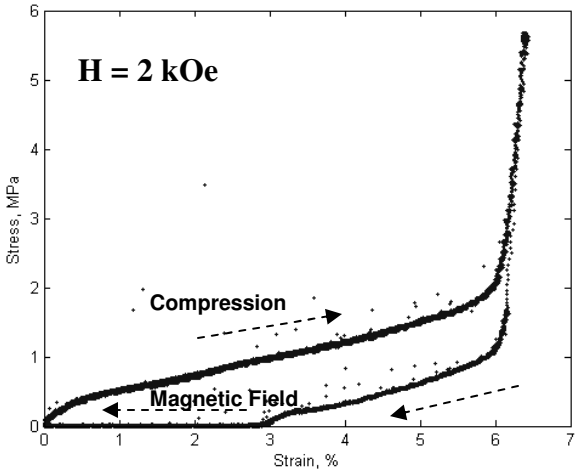


**Figure 2. Partial Pseudoelastic Behavior in NiMnGa.**

Because the mechanism of magneto-induced strains depends on the twinning and detwinning of martensite, it is necessary for the material to remain in the low temperature martensite phase. The MSM effect is not present in NiMnGa above the austenite finish temperature, $A_f$. As a result, care must be taken

to ensure that the material operates in a low temperature environment. For NiMnGa, the martensite to austenite transformation temperature occurs at 56°C, well above room temperature. In the context of the present work, all tests were conducted at room temperature to ensure that the actuator was completely in the martensite phase and that all strains observed are assumed to be the result of the magnetic shape memory effect.

For the purpose of establishing convention, external, constant applied fields refer to the field strength generated by the magnetic coil while the NiMnGa actuator is removed from the magnetic circuit. In other words, the mmf generated by the coils is held constant by controlling the drive current. It is difficult to measure the magnetic flux inside the NiMnGa sample due to the nature of the strain recovery mechanisms inherent to NiMnGa. To measure the magnetic flux inside the sample it is necessary to use a pickup coil. For active materials such as Terfenol, the direction of the strain response is parallel to the direction of the applied field. In this case, it is a relatively simple task to include a secondary, pickup coil between the active material and the primary magnetic coil. But in NiMnGa, the direction of strain is perpendicular to the direction of the applied field, therefore, introducing a pickup coil creates several complications. When the specimen is energized by the magnetic field, the natural tendency of the material is to expand along the long axis of the material. This axis is perpendicular to the direction of the field. For the pickup coil to measure the magnetic flux through the sample, it must also be oriented perpendicular to the magnetic field and wrapped around the specimen. This configuration creates a mechanical constraint that blocks the strain response of the material. In its current configuration, the use of a pickup coils is not feasible for these tests.

**Quasi-static Modeling of NiMnGa Actuators**

Because of the close similarities that exist between the behavior of NiTi and NiMnGa, it is necessary to consider the possibility that existing quasi-static phenomenological models for NiTi can provide a basis for MSMA modeling. There exist several, well-known examples of constitutive models used to predict thermal SMA behavior. The Tanaka, Liang and Rogers, Brinson, and Boyd and Lagoudas models are four well documented, SMA constitutive models. All four are similar, describing the material behavior in terms of three state variables: stress, strain, and temperature. These four models, the Brinson model in particular, are enormously useful in predicting NiTi SMA behavior. One of the key advantages of these models is that

since they rely on a series of experimentally determined material parameters, implementation is relatively straightforward. The proposed FSMA model is based on its own series of material parameters analogous to those in SMA models. Of the three NiTi models mentioned, the Brinson model is regarded as the most comprehensive and will be used to form the basis of the proposed quasi-static MSMA model.

The constitutive equation for the Brinson model using constant material functions is,

$$\sigma - \sigma_0 = E(\xi)(\varepsilon - \varepsilon_0) + \Omega_s(\xi_s - \xi_{s0}) + \Omega_T(\xi_T - \xi_{T0}) + \theta(T - T_0) \tag{1}$$

where E is the Young's modulus as a function of the martensite volume fraction, $\xi$, $\Omega_s$ and $\Omega_T$ are stress and temperature induced transformation tensors respectively, and $\theta$ is related to the thermal coefficient of expansion. The initial conditions, $\sigma_0$, $\varepsilon_0$, $\xi_{s0}$, $\xi_{t0}$, and $T_0$, are included. Similarly, the proposed NiMnGa quasi-static behavioral model takes the following form,

$$\sigma - \sigma_0 = E(\xi_\sigma)(\varepsilon - \varepsilon_0) + \Omega(\xi_\sigma)(\xi_\sigma - \xi_{\sigma 0}) + \lambda(\xi_{\sigma 0})(H - H_0) \tag{2}$$

where $\sigma_0$, $\varepsilon_0$, $\xi_{\sigma 0}$ , and $H_0$ represent the initial stress, strain, volume fraction of stress preferred martensite, and magnetic field intensity respectively. E, $\Omega$, $\lambda$ are constant material functions where E represents the Young's modulus of the MSMA, $\Omega$ is a transformation tensor, and $\lambda$ is related to the magnetostriction of the material. To better capture nonlinear effects in the material behavior, these material functions need not be constant and can be represented by higher order functions. To establish a convention, these material functions are defined in relation to the volume fraction of stress preferred martensite, $\xi_\sigma$. A magnetic field applied to the MSMA causes the volume fraction of stress preferred martensite to decrease resulting in the growth of field preferred martensite twins. This is analogous to the phase transition from martensite to austenite in NiTi SMA. However, as previously mentioned, strain recovery in thermal SMA occurs as a result of a phase transformation, while MSMA strain recovery occurs as a result of twin boundary motion in the martensite phase only. Therefore, the sum of the stress preferred martensite, $\xi_\sigma$, and field preferred martensite $\xi_H$ must always be equal to unity.

$$\xi_\sigma + \xi_H = 1 \tag{3}$$

If it is assumed that the material is at the maximum free strain condition, $\varepsilon = \varepsilon_L$, with the material initially composed entirely of the field preferred variant, $\xi_{\sigma 0} = 0$, with the initial conditions of $\sigma_0 = \varepsilon_0 = H_0 = 0$, and final conditions of $\xi_\sigma = 1$, $\varepsilon = \varepsilon_L$, and $\sigma = H = 0$, the following relation can be obtained:

$$\Omega = -\varepsilon_L E . \tag{4}$$

Using the constraint derived in (4), the FSMA constitutive equation may be reduced to the following, simplified form,

$$\sigma = E(\xi_\sigma)(\varepsilon - \varepsilon_L \xi_\sigma) + \lambda(\xi_\sigma)(H - H_0) \tag{5}$$

where $E(\xi_\sigma)$ is the Young's modulus of the material as a function of the stress preferred martensite volume fraction, $\varepsilon_L$ is the free-strain of the actuator, $\xi_s$ is the stress preferred volume fraction, $\lambda$ is related to the magnetostriction of the material and $H_0$ is the initial external field applied to the material.

The phenomenological model for NiMnGa describes the state of the material in terms of three state variables: stress, strain, and magnetic field. The model is characterized by nine experimentally determined constants. The nine parameters include: three material parameters: free strain, $\varepsilon_L$, stress preferred martensite Young's modulus, $E_\sigma$, field preferred martensite Young's modulus, $E_H$, two transition fields: $H_s$, $H_f$, two stress-influence coefficients: $C_s$, and $C_f$ and two fundamental critical stresses: $\sigma_{cr,s}$ and $\sigma_{cr,f}$. These parameters may be determined from testing the actuator over a range of constant, externally applied fields and observing the output stress and strain characteristics.

This report provides a summary of the work involved in the development of an FSMA model for NiMnGa. The present work deals primarily with the case of quasi-static actuation of the NiMnGa so dynamic effects have not yet been included. Dynamic modeling of FSMA actuator will be a topic for future investigation.

**Work Completed**

Samples of the NiMnGa alloy were obtained from the Finland based Adaptamat Company. The specimen used in this phase of testing was a 2x3x17 mm piece of single crystal martensite NiMnGa crystalographically oriented to produce strain in the long axis in response to an orthogonal magnetic field input.

A series of constant magnetic field tests were conducted in which the NiMnGa specimen was subjected to DC magnetic fields and then compressively loaded along the long axis of the specimen. To create a constant mmf environment in the magnetic circuit, the drive current in the coils was held constant. Initially, the specimen is induced into the field preferred configuration by applying a large, magnetic field at zero stress. Once the test begins, an increasing, compressive axial load is quasi-statically applied to the NiMnGa until the martensite twin variants of the material have been completely reordered into the stress preferred configuration. While the NiMnGa is still in the presence of the magnetic field, the stress is removed and the twin structure of the actuator is allowed to reach equilibrium. Stress and strain responses during the complete cycle were recorded and the critical transformation stresses were measured for each level of applied field. These stresses were then compiled into a critical stress vs. applied magnetic field profile. Model parameters were then identified from the critical stress vs. magnetic field profile and the stress-strain curves.

The test rig used in the constant applied external fields testing was designed and developed at the University of Maryland. Within this rig, the NiMnGa specimen was gripped between a 25 lb load cell and a moveable carriage. To ensure that the specimen was entirely exposed to the uniform field, it was carefully situated within the center of the air gap in the magnetic circuit. The carriage was driven by a NEMA-23 precision stepper motor and screw assembly. Axial loads were applied to the specimen by energizing the stepper motor and allowing it to compress the MSMA rod against the load cell at a prescribed strain rate. The accuracy of the load cell was within 0.0045 N. The magnetic field, B, was measured by a Hall sensor placed in the air gap between the specimen and pole face. Field intensity, H, and mmf were determined by calibrating the electromagnet with the level of current in the coils. Coil current was determined by measuring the voltage across a 1 ohm, precision resistor in series with the coil. Power to the coils of the electromagnet was provided by two 30V/10A DC power supplies. Actuator strain was determined by measuring the angular deflection of the motor with a potentiometer. The accuracy of the strain measurement is within 0.01 mm or 0.062 % strain. A photograph of the constant field test rig appears in Figure 3.

DC magnetic fields were applied to the NiMnGa by a laminated, transformer-steel core electromagnet capable of producing field intensities on the order of 10 kOe. The magnetic circuit is built

around a laminated core divided into two, E shaped halves, each consisting of 50 transformer steel layers. The halves are joined together by an aluminum frame and an air gap was machined out of the center bars of the E-frame to create magnetic poles. Two, 500 turn, copper wire coils, connected in parallel were fixed to the poles of the laminated core by interchangeable Delrin bobbins. The NiMnGa specimen is situated in between the two tapered poles of the electromagnet where a uniform, transverse field could be applied to the entire specimen. An air gap of approximately 0.030" exists between the NiMnGa specimen and the two pole faces.

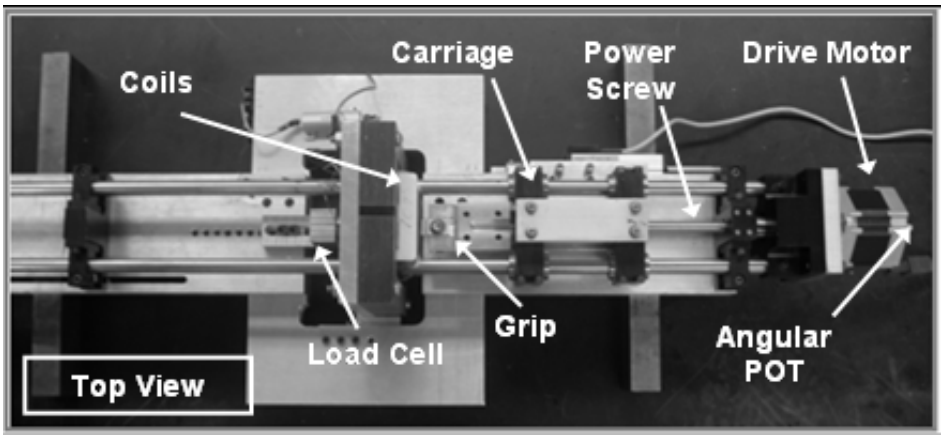


**Figure 3. Test rig for NiMnGa quasi-static testing.**

To ensure that a proper field distribution was applied along the length of the specimen, Hall effect sensors were used to characterize the uniformity of the field between the poles. The sensors were placed at regularly spaced intervals along the length of the NiMnGa actuator so that a profile of the field applied to the actuator could be developed. Based on this profile, the applied magnetic field varied less than 2% along the plane of the pole face and was assumed to be uniform for the purpose of these tests.

**Constant Magnetic Field Tests**

The first case, represented in Figure 4(a) illustrates the shape memory effect at zero applied field. Initially, the compressive stress is linearly related to the elastic deformation. When the axial stress reaches a critical value of $\sigma_1 = 0.3$ MPa in magnitude the twin boundaries in the martensite become mobile and the stiffness of the material is sharply decreased. While the twin boundaries are mobile, subsequent small increases in stress are accompanied by large increases in strain. The strains induced in this region are effectively plastic. When the level of stress reaches a second critical value, $\sigma_2 = 0.8$ MPa, the twin

boundaries in the material have been completely reordered into the stress preferred configuration and a sharp increase in material stiffness occurs. Further application of stress in this configuration yields elastic strain only. The maximum stress applied to the material in this test was 1.6 MPa. Removal of the stress in this state will produce a small amount of elastic recovery, approximately 0.2% in this case. The remaining 5.8% strain is plastic and recoverable only by the introduction of a magnetic field greater than 3.5 kOe. This magnetic shape memory effect behavior was observed for applied fields between 0 kOe and 1.5 kOe.

Figure 4(b) shows the second strain recovery behavior of the NiMnGa material, magnetic pseudoelasticity. In this instance, the external field level is 5 kOe. The loading behavior of the material follows the same pattern as that in the zero field behavior except that the first two critical transformation stresses are larger in magnitude. For a 5 kOe external field, these stresses are 2 MPa and 3.6 MPa for $\sigma_1$ and $\sigma_2$ respectively. After a maximum stress level of approximately 6 MPa is achieved, the stress is removed and the material initially recovers strain elastically. Because the material is exposed to a 5kOe magnetic field, the material begins a hysteretic recovery of strain at $\sigma_3$ when the load is removed. The twin boundary mobility is bounded by $\sigma_3$ and $\sigma_4$, 2.2 MPa and 0.72 MPa respectively. When the stress level is further decreased below $\sigma_4$ the remaining 0.4% strain in an elastic manner. All of the strain introduced into the NiMnGa upon loading is completely recovered in a hysteresis loop upon unloading, thus demonstrating the main characteristic of pseudoelastic behavior. The width of the hysteresis loop throughout the loading cycle is approximately 1 MPa. This pseudoelastic behavior was observed for all applied fields between 3.5kOe and 12 kOe.

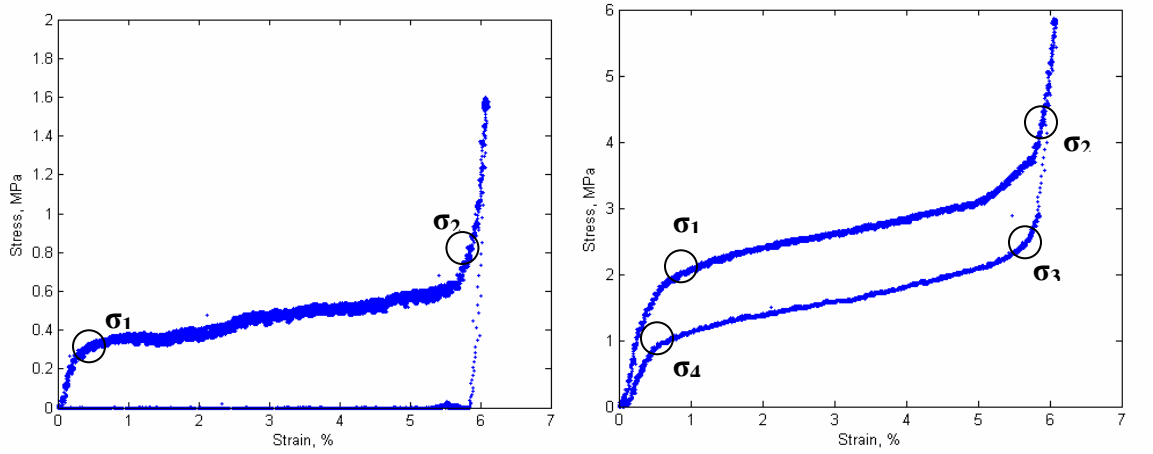


**(a) Magnetic shape memory at 0 kOe** **(b) Magnetic pseudoelasticity at 5 kOe**

**Figures 4. Common stress strain behaviors for NiMnGa.**

The third type of strain recovery involves a combination of both the previous behaviors at an intermediate applied field. When the compressive stress on the NiMnGa is removed, the material begins a pseudoelastic recovery of strain after $\sigma_3$ but the applied magnetic field is not sufficient to induce full twin boundary motion in the material. Thus, when the stress level reaches zero, a residual strain remains in the NiMnGa that can only be removed by adding additional magnetic field. Figure 5 illustrates partial magnetic pseudoelastic behavior for both a 2 kOe and 3 kOe applied fields. For a 2 kOe field, during unloading, when the compressive stress level drops below 0.8 MPa pseudoelastic recovery of strain begins to occur. However, when the stress level reaches zero, a residual strain of approximately 3% still remains within the material. When the level of applied field is raised further, the residual strain recovers in a manner similar to the zero-field magnetic shape memory effect. For a 3 kOe applied field, most of the strain, approximately 5% is recovered pseudoelastically, and a small residual strain of 0.5% remains when the load is completely removed. As in the case with the 2 kOe applied field, the residual strain is completely recovered by introducing a larger magnetic field. This behavior of partial pseudoelasticity was observed to occur for fields between 1.5 kOe and 3.5 kOe.

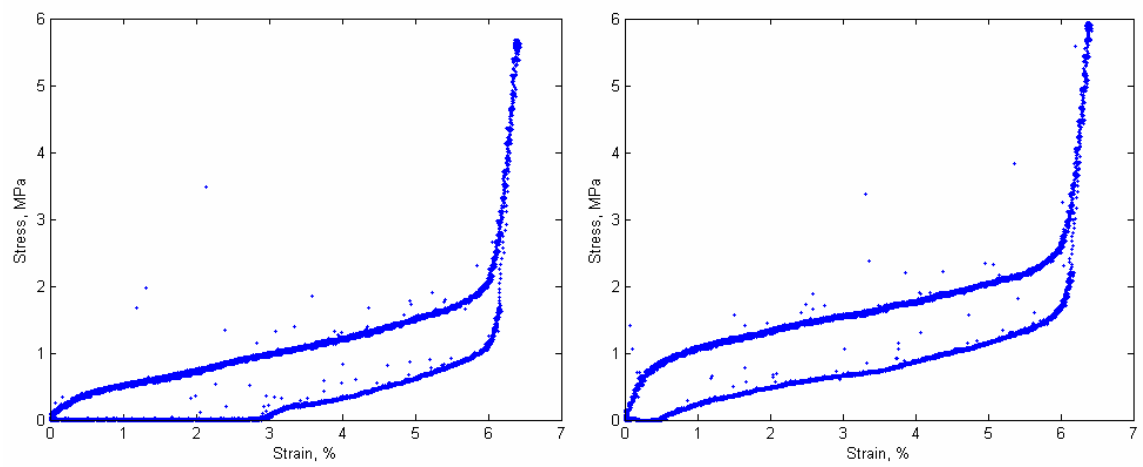


**(a) Applied Field: H = 2 kOe** **(b) Applied Field: H = 3 kOe**

**Figure 5. Partial pseudoelastic behavior in NiMnGa.**

For each level of applied field, the material behaves according to the same fundamental pattern. First, for a NiMnGa actuator initially in the field preferred state, the compressive stress is quasi-statically applied from 0 to 6 MPa, and a linear relation of stress to strain is observed in the beginning until a critical

level is reached ($\sigma_1 \approx$ 2-3 MPa). The stiffness of the material in this region, $E_H$, is the stiffness of the field preferred martensite variant of NiMnGa. Above this first critical stress level, $\sigma_1$, the material undergoes a rapid decrease in stiffness accompanied by a large increase in strain. In this region, twin boundary motion is induced and the material converts from the field to the stress preferred martensite variant. This behavior will continue until the material reaches a second critical stress, $\sigma_2$. Above this stress, the material has a volume fraction of stress preferred martensite equal to 1.0 and the stiffness increases sharply to $E_\sigma$, which is the stiffness of the stress preferred variant. When the load is removed from the material, similar critical stresses, $\sigma_3$ and $\sigma_4$, can be identified for the reverse transition from the stress to field preferred configuration. Figure 6(a) shows these parameters for the case of a 6 kOe external field.

The effect of increasing the applied field on the stress strain behavior of NiMnGa is shown in Figure 6(b). The main effect of increasing the field intensity is to raise the level of the critical stresses that mark the start and finish of twin boundary motion. The slopes of each stress-strain curves before $\sigma_1$, and after $\sigma_2$ do not appear affected by the change in magnitude of applied field. This leads to the conclusion that despite the level of field, the stiffness of the material when in the field or stress preferred configuration remains unchanged. In contrast, the critical transformation stresses show a pronounced dependence on the applied magnetic field.

**Parameter Identification**

There are nine model parameters that must be quantified in order to characterize the quasi-static model. The first three parameters, $E_\sigma$, $E_H$, and $\varepsilon_L$, are obtained from direct examination of the stress-strain curves of the constant applied field tests. From the data in Figure 6, the Young's modulus for the field preferred variant, $E_H$ is 450 MPa, while the Young's modulus for the stress preferred variant, $E_\sigma$ is 820 MPa. Since these values do not show a pronounced dependence on applied field, they are considered constants. The free strain parameter, $\varepsilon_L$ can be determined from Figure 4(a). The magnitude of plastic strain remaining in the material after the load has been removed in a zero field environment is 5.8%. This amount of residual strain is the free strain of the MSMA and represents the maximum strain capability of the material.

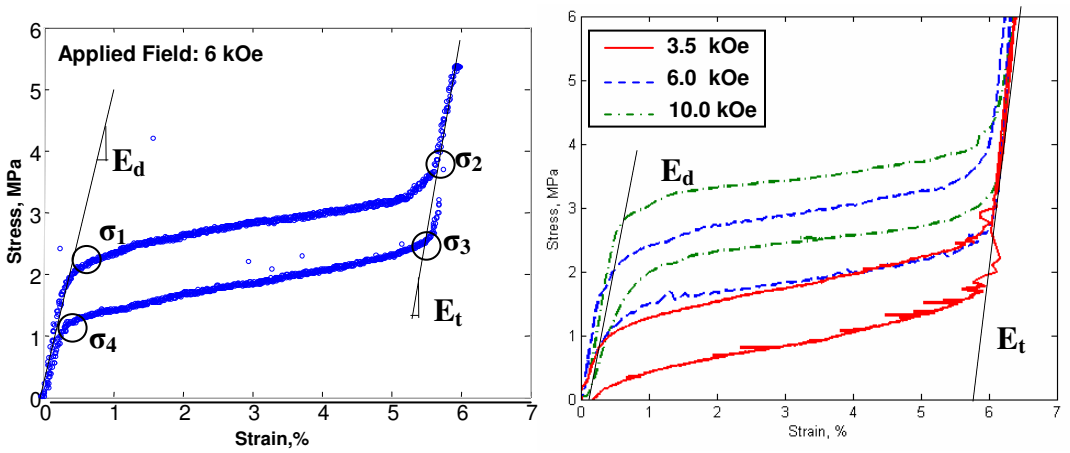


**(a) Critical stresses and Young's moduli** **(b) Comparison of behavior at different fields**

**Figure 6. Effect of applied field on stress-strain behavior of NiMnGa.**

The final six parameters are quantified by closely studying the relation between the four critical transformation stresses and the applied field. By identifying the critical stresses over a range of field intensities, a critical stress profile, shown in Figure 7, can be developed for an iso-magnetic field. The beginning and end of the twin boundary motion during loading are denoted as $\sigma_1$ and $\sigma_2$, respectively. For twin boundary motion during recovery, $\sigma_3$ and $\sigma_4$ are similarly defined. Each curve of the critical stress behavior is linearly related to applied field below 7 kOe. For external fields larger than 7 kOe, the critical stresses begin to level off, indicating the onset of magnetic saturation. Because the $\sigma_1$ and $\sigma_3$ curves are coincident and the $\sigma_2$ and $\sigma_4$ curves are parallel, it is sufficient to define, two, linear stress influence coefficients. The first stress influence coefficient, $C_s$, is defined as the slope of the $\sigma_1$ and $\sigma_3$ curves, or in other words, the variation of critical stress with applied field for the beginning of twin boundary motion. The second stress influence coefficient representing the critical stress behavior at the end of twin boundary motion, $C_f$, is determined from the slope of the $\sigma_2$ and $\sigma_4$ curves. Also, since this is a linear model, higher order effects like magnetic saturation, are neglected for now but will be revisited later. Each coefficient has units of MPa per kOe. Based on the experimental data, the values for $C_s$ and $C_f$ are 0.452 MPa/kOe and 0.488 MPa/kOe respectively.

The critical stress profile also provides the remaining four model parameters. First, the points corresponding with zero applied field of the $\sigma_1$ and $\sigma_2$ curves are the two fundamental critical stresses $\sigma_{cr,s}$ and $\sigma_{cr,f}$. These fundamental stresses define the region of twin boundary motion at zero applied field. Along with the appropriate stress influence coefficients, these parameters can be used to predict the critical

stresses for any applied field during the loading cycle. These fundamental critical stresses are 0.284 MPa and 0.902 MPa for $\sigma_{cr,s}$ and $\sigma_{cr,f}$ respectively. The critical stresses of the reverse transition, $\sigma_3$ and $\sigma_4$, exist only above certain threshold fields. By noting the x-intercepts of these two curves, the two fundamental threshold fields, $H_s$ and $H_f$ may be identified. In addition to being useful for determining critical transformation stresses, these two parameters mark the regions where the SME, partial pseudoelasticity, and pseudoelasticity behaviors occur. For instance, the x-intercept of the $\sigma_3$ curve and the value for the $H_s$ parameter is 1.0 kOe. For applied fields less than 1.0 kOe, there will be no pseudoelastic recovery in the NiMnGa upon unloading. Therefore, the only mechanism for strain recovery in this region is the SME. Likewise, the $H_f$ field is defined as the x-intercept of the $\sigma_4$ curve, which is 3.5 kOe. So, for applied fields greater than 1.0 kOe but less than 3.5 kOe, the actuator will begin to revert back to the field preferred configuration during unloading but will still retain some amount of residual strain when the load is completely removed. This region between $H_s$ and $H_f$ is where the phenomenon of partial pseudoelasticity occurs. It follows then that for field greater than $H_f$, 3.5 kOe, the main strain recovery mechanism will be magnetic pseudoelasticity. A summary of all the model parameters is shown in Table 1.

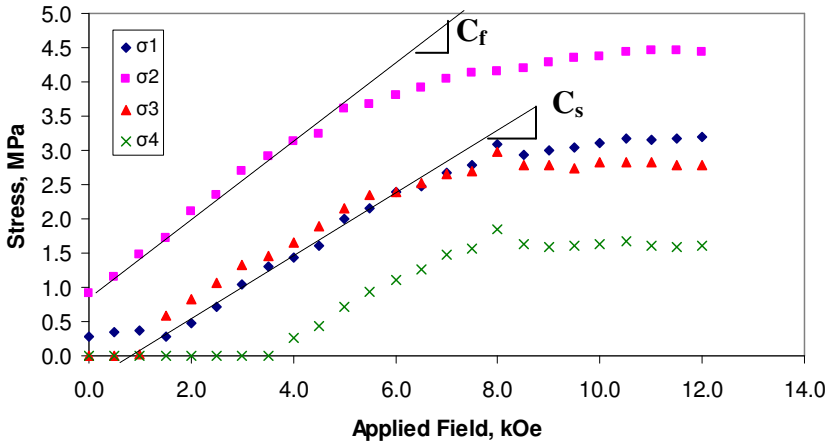


**Figure 7. Critical Stress vs. Applied Field profile.**

**FSMA Quasi-Static Model Validation**

Once the model parameters are identified, the quasi-static model may be implemented and validated with experimental data. In the model, stress is calculated in the actuator for a discrete number of strain steps. Once the stress reaches a predicted critical stress, twin boundary motion occurs. As mentioned

previously, these critical stresses are functions of applied magnetic field and can be determined from the corresponding combination of the parameters $\sigma_{cr,s}$, $\sigma_{cr,f}$, $C_s$, $C_f$, $H_s$, and $H_f$. During the region of twin boundary motion, a linear function is used to describe the transformation from the stress to field preferred martensite configurations. The first benchmark for a successful NiMnGa behavioral model is that it must be able to capture all of the major strain recovery mechanisms of the material including the magnetic shape memory effect, partial pseudoelasticity, and pseudoelasticity. In Figure 8(a), the result from the analytical model is compared to the experimental stress-strain curve for the zero field condition to show the model's effectiveness at capturing the magnetic shape memory effect. Figure 8(b) shows the results of the model compared to the stress-strain curve for a specimen exposed to a constant 5 kOe field, demonstrating the model's ability to capture magnetic pseudoelastic behavior.

**Table 1. Experimentally determined FSMA quasi-static model parameters.**

| Parameter | Value | Units |
|---|---|---|
| $H_s$ | 1.0 | kOe |
| $H_f$ | 3.5 | kOe |
| $\sigma_{cr,s}$ | 0.284 | MPa |
| $\sigma_{cr,f}$ | 0.902 | MPa |
| $C_s$ | 0.452 | MPa/kOe |
| $C_f$ | 0.488 | MPa/kOe |
| $E_\sigma$ | 820 | MPa |
| $E_H$ | 450 | MPa |
| $\varepsilon_L$ | 5.8 | % |

In general, the model shows good agreement with the experimental data in Figure 8. Critical threshold stresses are predicted with a reasonable degree of accuracy and the model seems to capture both of the primary strain recovery mechanisms of the actuator. In the pseudoelastic region there is a tendency of the model to slightly over-predict stresses during loading and slightly under-predict stresses during unloading. Generally, these inconsistencies are small and do not seriously undermine the accuracy of the analysis. The model does not, however, incorporate the smooth transitions between the field and stress preferred martensite configuration. This result is expected in a piecewise linear model, however, and further refinement is necessary to include higher order effects.

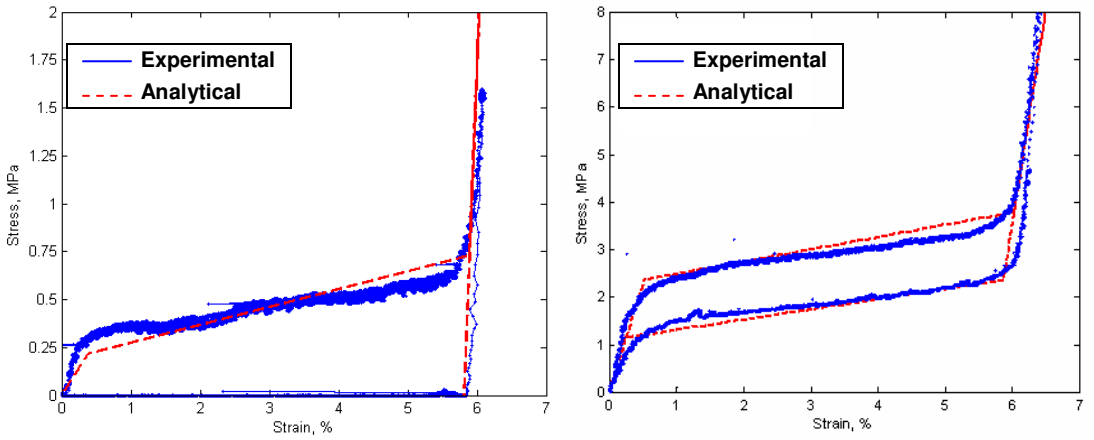


**(a) SME at O kOe applied field** **(b) Pseudoelasticity at 5 kOe applied field**

**Figure 8. Comparison of experimental data and theoretical model for common strain recovery mechanisms.**

For further validation, a comparison between the model and experimental data of non-standard strain recovery behavior is necessary. In Figure 9(a) the ability of the model to predict partial pseudoelasticity is shown. Although the general shape of the NiMnGa behavior is reflected in the model, inconsistencies in stress calculation during the loading and unloading cycles are much more pronounced than they were in the cases shown in Figure 8. The model over-predicts the stresses during twin boundary motion by as much as 20% during the loading cycle for the partial pseudoelastic case shown in Figure 9(a). Although the predicted stresses during unloading are better, there still exists a higher degree of model error than seen in the pseudoelastic analysis. Figure 9(b) shows a comparison between the analytical model and a minor hysteretic loop at 6 kOe. Like all of the previous cases, the model is capable of predicting the stress-strain curves of minor loops. For both partial pseudoelasticity and minor loops, the linearity of the model neglects higher order material behavior, which leads to errors in the approximation of the stresses associated with twin boundary motion. These discrepancies lead to slightly less desirable predictions than in the cases of the SME and pseudoelasticity. Although useful for providing a general picture of actuator behavior, the linear model requires further refinement before it can accurately predict material behavior at these intermediate states.

One of the underlying assumptions of the model is that all parameters are linearized. As a result, higher order effects such as magnetic saturation are neglected. This means that the analytical model will over-predict the critical stresses for large external fields close to saturation. Figure 10(a) demonstrates this

limitation by comparing the model to the experimental stress-strain curve for a 8 kOe external field. Clearly, the model does not accurately capture the physical behavior of the material in this case. When the applied field is larger then 7 kOe, the NiMnGa begins to saturate. At the onset of magnetic saturation, the material no longer maintains a linear relationship between critical transformation stresses and applied field. Since the model initially uses linear stress-influence coefficients, they are insufficient for predicting critical stresses at or near magnetic saturation. What is now required is a new set of functions to replace the linearized coefficients $C_s$ and $C_f$. These functions can be obtained from the critical stress profile shown in Figure 7. When $C_f$ and $C_s$ are expanded from linear coefficients to simple, third order polynomials they improve the ability of the model to predict critical stresses for any external magnetic field. These following expressions represent the nonlinear equations and conditions used to calculate critical transformation stresses in the NiMnGa.

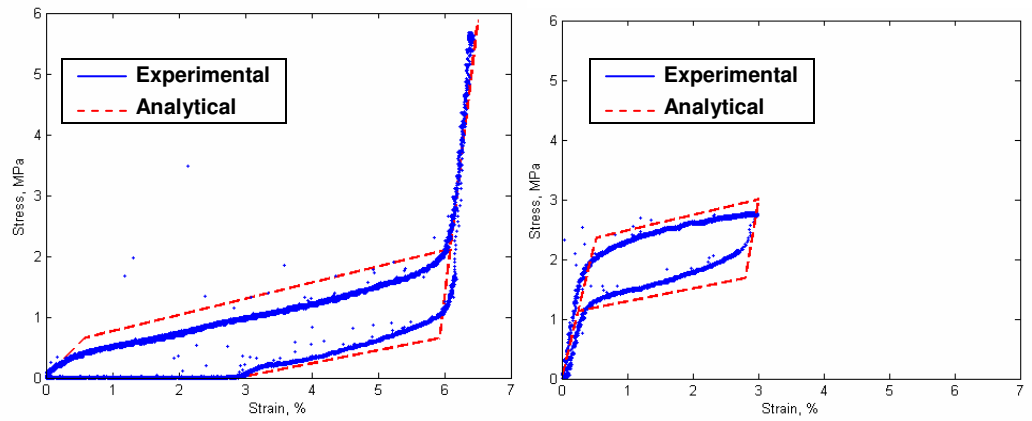


**(a) Partial pseudoelastic recovery at 2 kOe** **(b) Minor loop behavior at 6 kOe**

**Figure 9. Comparison of experimental data and theoretical model for various non-standard behaviors.**

For pseudoelastic behavior ($H_{applied} > H_f$ ),

$$\sigma_1 = \sigma_3 = \left(-0.0002 * H_{applied}^3 - 0.0289 * H_{applied}^2 + 0.6678 * H_{applied} - 0.5614\right) * 10^6 \quad (7)$$

$$\sigma_2 = \left(0.0005 * H_{applied}^3 - 0.0399 * H_{applied}^2 + 0.699 * H_{applied} + \sigma_{cr,f}\right) * 10^6 \quad (8)$$

$$\sigma_4 = \left(0.0024 * H_{applied}^3 - 0.1024 * H_{applied}^2 + 1.292 * H_{applied} - 3.441\right) * 10^6 \quad (9)$$

For the partial pseudoelastic behavior ($H_s > H_{applied} > H_f$),

$$\sigma_4 = 0 \quad (10)$$

For shape memory behavior ($H_{applied} < H_s$),

$$\sigma_3 = \sigma_4 = 0 \tag{11}$$

$$\sigma_1 = \sigma_{cr,s} \tag{12}$$

In Figure 10(b), the model is once again compared to the experimental stress-strain curve for a 8 kOe external field. In this case, however, the model has been updated to include higher order critical stress functions. The critical stresses are not over-predicted in Figure 10(b) as they were in 10(a), therefore, the model is able to compensate for the effects of magnetic saturation and yields a better prediction of material behavior.

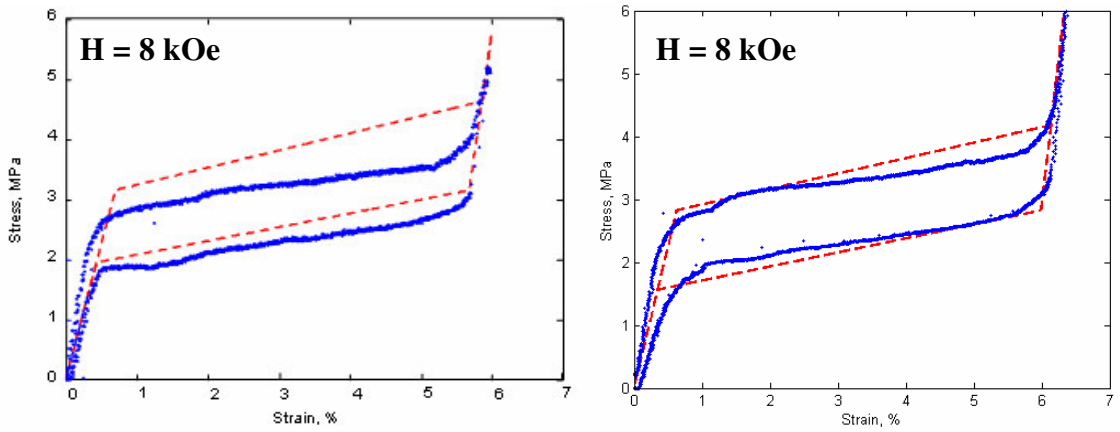


**(a) Linear stress influence coefficients** **(b) Non-linear stress influence coefficients**

**Figure 10. Effect of linear stress influence coefficients and magnetic saturation.**

## Future Work

The development of a comprehensive behavioral model for NiMnGa is currently underway. Although a good correlation exists between the calculated results and the test data, there are several issues that must be addressed in order to further improve the accuracy of the quasi-static model. Most important is that since the model is based on a piecewise linear formulation, it does not accurately capture the smooth transitions of the stress-strain behavior at the beginning and end of twin boundary motion. Further refinements are necessary in order to resolve this issue. Now that material behavior under a constant drive current has been evaluated, the next step is to observe the material behavior while the flux in the magnetic circuit is kept constant. Future tests will involve compression of the NiMnGa in a constant magnetic flux environment. Finally, the quasi-static model will be extended to capture the dynamic behavior of the MSMA so that it may be used to develop smart actuators for a range of applications.